

Accurate mapping of Chinese coastal aquaculture ponds using biophysical parameters based on Sentinel-2 time series images

Ya Peng, Dhritiraj Sengupta, Yuanqiang Duan, Chunpeng Chen, Bo Tian *

State Key Laboratory of Estuarine and Coastal research, East China Normal University, Shanghai 200241, China



ARTICLE INFO

Keywords:
Aquaculture ponds
Remote sensing
Google Earth Engine
Time series
Chlorophyll-a

ABSTRACT

Aquaculture plays a crucial role in the global food security and nutrition supply, where China accounts for the largest market share. Although there are some studies that focus on large-scale extraction of coastal aquaculture ponds from satellite images, they have often variable accuracies and encounter misclassification due to the similar geometric characteristics of various vivid water bodies. This paper proposes an efficient and novel method that integrates the spatial characteristics and three biophysical parameters (Chlorophyll-a, Trophic State Index, and Floating Algae Index) to map coastal aquaculture ponds at a national scale. These parameters are derived from bio-optical models based on the Google Earth Engine (GEE) cloud computing platform and time series of high-resolution Sentinel-2 images. Our proposed method effectively addresses the misclassification issue between the aquaculture ponds and rivers, lakes, reservoirs, and salt pans and achieves an overall accuracy of 91 % and a Kappa coefficient of 0.83 in the Chinese coastal zone. Our results indicate that the total area of Chinese coastal aquaculture ponds was 1,039,214 ha in 2019, mainly distributed in the Shandong and Guangdong provinces. The highest aquaculture intensity occurs within the 1 km coastal buffer zone, accounting for 22.4 % of the total area. Furthermore, more than half of the Chinese coastal aquaculture ponds are concentrated in the 0–5 km buffer zone. Our method is of general applicability and thus is suitable for large-scale aquaculture ponds mapping projects. Moreover, the biophysical parameters we employ can be considered as new indicators for the classification of various water bodies even with different aquaculture species.

1. Introduction

Aquatic food plays a significant and growing nutritional role and is considered an essential enabler for securing the global Sustainable Development Goals (SDGs). During the last couple of decades, the depletion of wild fishery resources has promoted the vigorous development of aquaculture (Ottinger et al., 2016). It is estimated that the global fish production reached 179 million tons in 2018, of which 82 million tons were produced by aquaculture. This accounts for 46 % of the total production and 52 % of the fish used for human consumption (FAO, 2020). The demand for fish production continues to increase. Recent studies predict that the proportion of the human population living in Low Elevated Coastal Zones (LECs) will increase from 58 % to 71 % by 2050, exceeding one billion (Merkens et al., 2016). Hence, more coastal residents in the world have opted for aquaculture to satisfy their current and future food demands. In 2010, the area used for aquaculture in the coastal zone exceeded 6000 km², accounting for about 30 % of the global aquaculture (Waite et al., 2014). To improve aquaculture

production, much of the coastal land has been irreversibly altered (Chen et al., 2017; Páez-Osuna, 2001). A recent study reports that about 22 % of the reclamation land on the Chinese coast has been converted to aquaculture ponds (Duan et al., 2021). Furthermore, the rapid expansion of coastal aquaculture has also resulted in large-scale wetlands fragmentation and loss (Peng et al., 2013; Spalding et al., 2014) that seriously damaging the coastal ecosystems. Additionally, the use of fertilizers and antibiotics for enriching the waters and preventing bacterial infections in aquaculture ponds, contributes to water pollution and food security problems due to the discharge of the produced sewage (Ottinger et al., 2016; Sohel and Ullah, 2012). Therefore, quantitative assessment of the spatial scope and distribution of aquaculture ponds on a large scale is of great significance in providing a high accurate database for efficiently evaluating wetland habitats loss and its impact on the marine environment.

A considerable amount of literature has been published on mapping and detection of aquaculture from satellite data (Føre et al., 2018). For instance, based on SPOT-5 and WorldView-1 panchromatic images,

* Corresponding author.

E-mail address: btian@sklec.ecnu.edu.cn (B. Tian).

Virdis (2014) identified coastal aquaculture in the Tam Giang-Cau Hai Lagoon area using region-growing segmentation and unsupervised clustering classifier ISOSEG. **Yao et al. (2016)** provided a systematic analysis of the temporal and spatial distribution of Chinese coastal salt pans and aquaculture ponds from 1985 to 2010 based on Landsat TM/ETM+ images. **Ottinger et al. (2018)** used time series of Sentinel-1 SAR data to map the aquaculture ponds in several locations across coastal Asia. Employing also Sentinel-1 SAR data, **Sun et al. (2020)** constructed a national-scale automatic extraction algorithm for aquaculture ponds based on the comprehensive water index, texture, and geometric information, and successfully verified their results via experiments on the coastal areas of Vietnam.

Remote sensing classification methods have been also widely used in aquaculture ponds extraction. Compared to traditional visual interpretation methods (**Yao et al., 2016**), machine learning have been widely used in the identification of aquaculture ponds. For instance, **Tran et al. (2015)** adopted a maximum likelihood classifier to obtain the land cover and use dynamics in the Mekong Delta of Vietnam, where aquaculture pond is considered as one of the land types. Using high-resolution infrared images, **Zeng et al. (2021)** established a deep learning model based on a fully convolutional neural network for detecting inland aquaculture ponds. Furthermore, given the typical man-made features of aquaculture ponds, object-based classification methods have been commonly used in their identification. For example, **Ren et al. (2019)** used an integrated updating and object-oriented classification method to map the coastal aquaculture ponds in China from 1984 to 2016, with a 30 m spatial resolution of Landsat images. **Ying et al. (2020)** used object-oriented classification on SPOT-5 (with 2.5 m spatial resolution) and GF-1 (with 2 m spatial resolution) satellite images to detect changes in coastal aquaculture areas of southeastern China.

Cloud computing platforms such as Google Earth Engine (GEE) have also significantly contributed to the large-scale identification of aquaculture ponds. **Xia et al. (2020)** extracted the aquaculture ponds of Shanghai in the 2016–2019 period using Multi-threshold Connected Component Segmentation and a Random Forest algorithm by integrating multi-source remote sensing data on the GEE. **Duan et al. (2020)** utilized a decision tree and Landsat data together with GEE, to automatically identify large-scale aquaculture ponds in Coastal China.

While many achievements have been made concerning the mapping and dynamic monitoring of coastal aquaculture ponds, most of the above-mentioned studies focus on spatial, spectral, and geometric characteristics. Far too little attention has been paid to the misclassification between aquaculture ponds and other types of land use that have similar shapes, e.g., paddy fields, bare lands, lakes, reservoirs, and salt pans. This misclassification is mainly due to the drainage of aquaculture ponds during non-farming seasons and the coarse resolution of satellite images. To the best of our knowledge, there is no study that has applied a targeted approach to eliminate objects that have similar spatial features to aquaculture ponds.

Fertilizing aquaculture ponds increases the production of the natural ingredients that feed the fish, shrimp, crab, and other aquatic organisms. This however changes the water quality. In this paper, we incorporate the high-nutritional characteristics of aquaculture ponds to improve their mapping accuracy. To do this, we consider three biophysical parameters derived from time series of Sentinel-2 images. By quantifying these biophysical parameters, namely Chlorophyll-a (Chl-a), Trophic State Index (TSI) and Floating Algal Index (FAI) over different water bodies, we advance the automatic identification of coastal aquaculture water by distinguishing it from other neighboring land uses. Based on the proposed method, we complete the mapping and analysis of the spatial pattern and distribution of Chinese aquaculture ponds existing in 2019. Our results provide a new perspective on remote identification of aquaculture ponds. The proposed method has the ability of distinguishing high-nutrition aquaculture water from other water bodies such as rivers, lakes, reservoirs, and salt pans, even among different aquaculture species.

2. Study area and materials

2.1. Study area

China accounts for more than 50% of the global aquaculture food production (FAO, 2020). Out of this, the aquaculture ponds are the main source of aquatic food (China Fishery Statistical Yearbook, 2020; Duan et al., 2020). The coastal zone, where terrestrial and oceanic ecosystems interact, is the most densely populated and socioeconomically developed region in China. It accommodates 43.5 % of the country's population and produces 60.8 % of the gross domestic product (GDP) (Wang et al., 2014). The low-lying coastal areas have densely intertwined river networks, which developed a large number of estuarine deltas (e.g. the Yellow River Delta, the Changjiang River Delta, and the Pearl River Delta) and vast tidal flats (e.g. the North Jiangsu Coastal Plain). These areas provide suitable conditions for the large-scale establishment of aquaculture ponds. Hence, we selected the Chinese coastal zone as our study area. The aquaculture ponds in Chinese coastal zone are diverse in types and aquaculture patterns, and different types have distinct geometric and biophysical characteristics. The intensive grid structure made the aquaculture pond regions different from other water bodies like lakes, rivers and reservoirs.

The vast terrain and underground brine resources of Chinese coastal zone also provide a suitable environment for the development of salt pans. Most of the salt pans consist of evaporation and crystallization ponds, with drainage pools that can also be used for aquaculture.

For a detailed analysis of the distribution of aquaculture ponds in Chinese coastal zones, we consider all coastal counties that intersect with the 30 km buffer along the Chinese administration coastline. This area spans a region from the northernmost province, Liaoning (43°N, 125°E), to the southernmost, Hainan (18°N, 108°E), covering approximately 25 degrees of latitude and 17 degrees of longitude, and including 10 provinces (Liaoning, Hebei, Shandong, Jiangsu, Zhejiang, Fujian, Guangdong, Guangxi, Hainan, Taiwan), two municipalities (Tianjin, Shanghai), two special administrative regions (Hong Kong, Macao). This covers a total of 311 coastal counties, cities, and districts (Fig. 1).

2.2. Materials

The images used in this paper include Sentinel-2 Level-2A Surface Reflectance data and Level-1C Top of Atmosphere Reflectance data from the US Geological Survey (USGS) Center for Earth Resources Observation and Science (<http://glovis.usgs.gov/>). All the images available on GEE are orthorectified and geometrically corrected. Additionally, the Level-2A Surface Reflectance data was atmospherically corrected using the Sen2Cor processor (Louis et al., 2019).

The Sentinel-2 environmental monitoring satellite is a wide-swath, multispectral imaging mission for earth observation launched by the European Space Agency (ESA). It includes two multispectral satellites A and B, which were launched on June 23, 2015, and March 7, 2017, respectively. Sentinel-2A and 2B have the same orbit and provide repeated observations with a five-day revisit period. This enables frequent and large-scale mapping and monitoring of the coastal aquaculture ponds. The 10–20 m spatial resolution of Sentinel-2 images considerably improves the accuracy of aquaculture ponds identification (Table 1).

The Multi-Error-Removed Improved-Terrain Digital Elevation Model (MERIT DEM) taken from Shuttle Radar Topography Mission (SRTM) (SRTM, 2017) are used to identify the low-lying coastal zones. MERIT DEM is a high accuracy global DEM at 3 arc sec resolution (~90 m at the equator) produced by eliminating major error components from existing DEMs.

The imagery used for the validation of our identification method includes the ground survey images captured by DJI Drone Phantom-4 RTK and the high-resolution images collected from Google Earth. These high-resolution drone images were captured during 2018–2020,

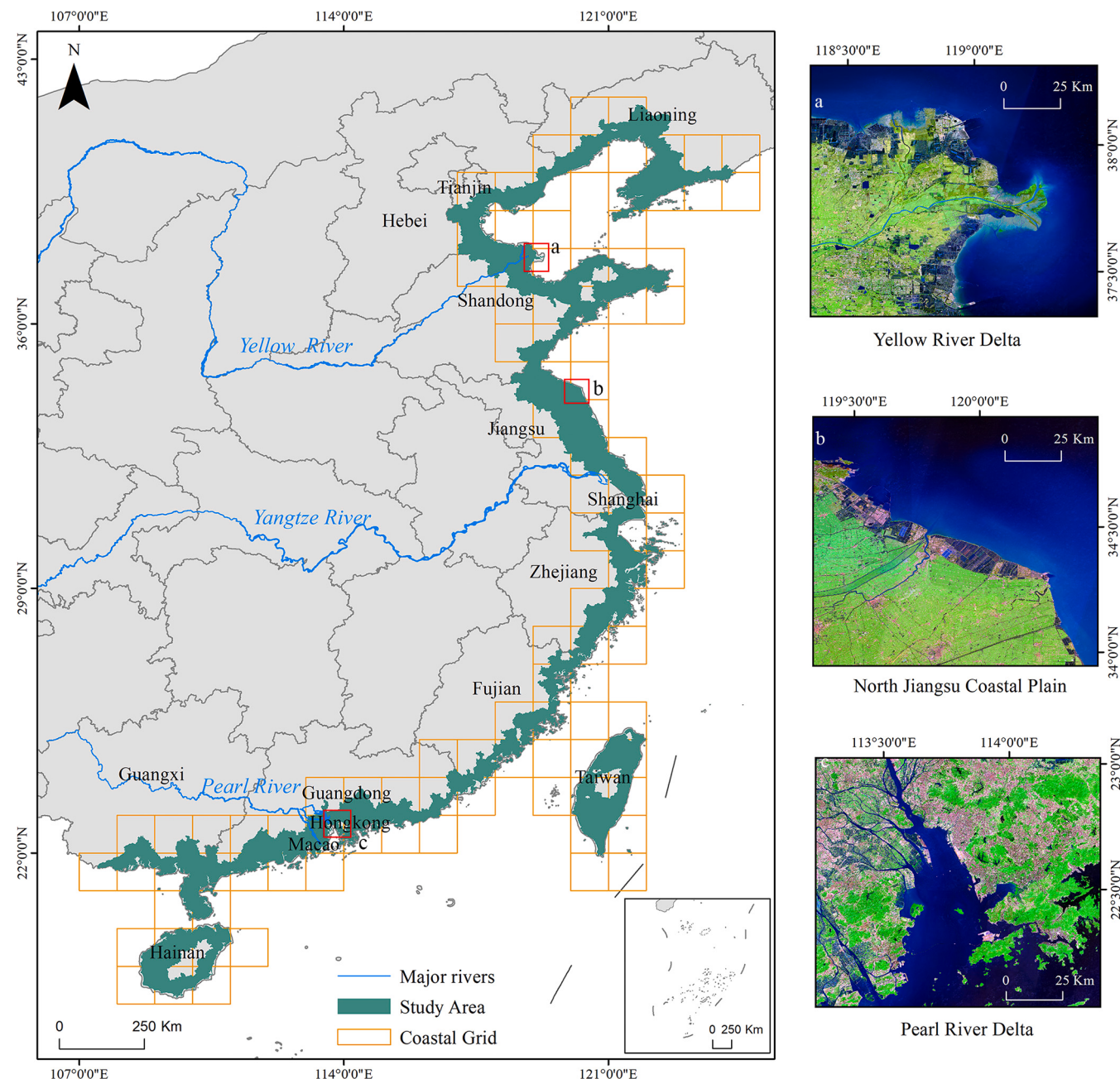


Fig. 1. The study area.

which including latitude and longitude information. For the locations where there is no drone photos, we collected high-resolution validation points from Google Earth to conduct the accurate verification.

3. Methodology

Our method is built upon the spatial characteristics of Chinese coastal aquaculture ponds and the differences between the biophysical parameters of various types of water. To facilitate the extraction of coastal water bodies and the retrieval of biophysical parameters. All Sentinel-2 images are processed using the quality band (QA60 bands in Sentinel-2) to mask out clouds after filtering the images with less than 20 % of cloud cover in the GEE platform. As aquaculture ponds are mainly distributed in low-lying coastal plains, therefore, the SRTM elevation data lower than 20 m is used to acquire low-lying coastal areas and reduce computational capacity.

The Sentinel-2 time-series and the decision tree classifier are used to extract the aquaculture ponds in our study area. The water index and thresholding methods are constructed to extract the coastal water bodies, these extracted water bodies include aquaculture ponds, lakes, reservoirs, and salt pans, etc. Besides, we adopt morphological operations to combine the aquaculture pond regions and remove the individual pixels or small areas on water body polygons. Images of the yearly mean value of Chl-a, TSI and FAI are then derived from the aggregation of Sentinel-2 time series using the GEE platform. Then we use the Zonal Statistics spatial analysis tool in ArcGIS to extract mean biophysical parameters of each water polygon. Finally, we chose different types of water samples from Google Earth high-resolution imagery and field survey, including aquaculture ponds, lakes, rivers, reservoirs, and salt pans to decide the optimal threshold of aquaculture ponds extraction. These are used to establish the decision rule for extracting aquaculture ponds (Fig. 2).

Table 1
Dataset used for aquaculture mapping.

Process	Dataset	Bands	Central Wavelength (nm)	Resolution (m)
Waterbody extraction	Sentinel-2	Green:B3	560.0(S2A)/559 (S2B)	10
		Red: B4	664.5(S2A)/665 (S2B)	10
		Red Edge1: B5	703.9(S2A)/703.8(S2B)	20
		NIR: B8	835.1(S2A)/833S2B)	10
		Red Edge4: B8A	864.8(S2A)/864 (S2B)	20
		SWIR1: B11	1613.7(S2A)/1610.4(S2B)	20
		SRTM, 2017	/	3 arc sec
		Red Edge1: B5	703.9(S2A)/703.8(S2B)	20
		Red: B4	664.5(S2A)/665 (S2B)	10
		NIR: B8	835.1(S2A)/833S2B)	10
Biophysical parameters retrieval	Sentinel-2	SWIR1: B11	1613.7(S2A)/1610.4(S2B)	20

3.1. Water body extraction

To accurately extract water surfaces from remote sensing imagery, researchers construct water index to delineate open water features through a band-ratio approach. Water index method has been widely used in extracting water bodies, for it can highlight the spectral difference between water and non-water surfaces.

To improve the accuracy of coastal water bodies extraction, in this paper, we test six different water indices by collecting different

aquaculture ponds areas. The six water indices include the Normalized Difference Water Index (NDWI) (McFeeters, 1996), the Modified Normalized Difference Water Index (MNDWI) (Xu, 2006), two Automated Water Extraction Index (i.e., AWEInsh and AWEIsh) (Feyisa et al., 2014), Water Index (WI₂₀₁₅) (Fisher et al., 2016), and the Multi-Band Water Index (MBWI) (Wang et al., 2018) (Table 2). The Otsu method (Otsu, 1979), widely used for water body extraction, is adopted to automatically determine the extracting threshold.

Different aquaculture ponds areas were collected to calculate the Relative Error (RE) using Eq. (1)

$$RE = \frac{(\text{Area}_{\text{water index}} - \text{Area}_{\text{aquaculture ponds}})}{\text{Area}_{\text{aquaculture ponds}}} \quad (1)$$

The RE values for NDWI, MNDWI, AWEInsh, AWEIsh, WI₂₀₁₅, and MBWI are 4.47, 3.21, 8.29, 8.22, 7.50, and 3.72, respectively. As it is seen, AWEInsh, AWEIsh and WI₂₀₁₅ provide low performance in distinguishing water bodies. Furthermore, the results show that NDWI mistakenly classifies bare land as water bodies.

In the results of water bodies extraction, MNDWI and MBWI show

Table 2
Accuracy assessment of water bodies extraction by various water indices.

Index	Equation	Relative Error
NDWI (McFeeters, 1996)	(G-NIR)/(G + NIR)	4.47
MNDWI (Xu, 2006)	(G-SWIR1)/(G + SWIR1)	3.21
AWEInsh(Feyisa et al., 2014)	4(G-SWIR1)/(0.25NIR + 2.75SWIR2)	8.29
AWEIsh(Feyisa et al., 2014)	B + 2.5G-1.5(NIR + SWIR1)-0.25SWIR2	8.22
WI ₂₀₁₅ (Fisher et al., 2016)	1.7204 + 171G + 3R-70NIR-45SWIR1-71SWIR2	7.50
MBWI (Wang et al., 2018)	2G-R-NIR-SWIR1-SWIR2	3.72

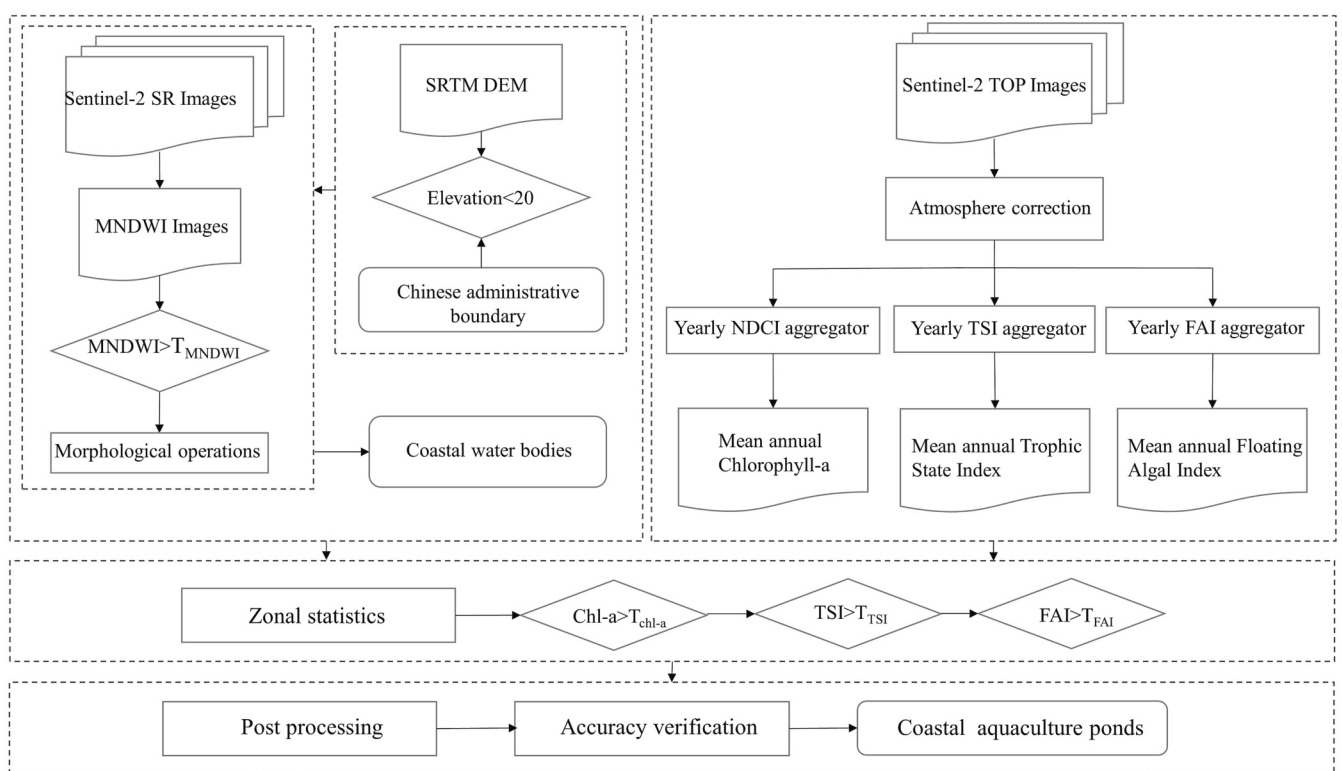


Fig. 2. Workflow used in our extraction method (MNDWI: Modified Normalized Difference Water Index; NDCI: Normalized Differential Chlorophyll Index; Chl-a: Chlorophyll-a; TSI: Trophic State Index; FAI: Floating Algal Index).

reasonable levels of accuracy, however, MBWI is very sensitive to the changes in internal water pixels of aquaculture ponds polygons. This results in multiple holes within a single water polygon. Among the above-named indices, MNDWI is the most efficient with the highest extraction accuracy, and capable of efficiently distinguishing paddy fields and built-up areas (Fig. 3). Furthermore, MNDWI shows higher stability in the extraction of coastal water bodies with the extraction threshold concentrated in the -0.2 to 0.2 range. Based on the above results, we use the MNDWI to extract coastal water bodies in this paper.

Aquaculture ponds are essentially artificial or natural closing water bodies filled with water for a long time. Nevertheless, during the harvest season, some aquaculture ponds might become partially or fully dry (Ottinger et al., 2017). For example, shrimp ponds have a large amount of drainage in winter and spring (usually between November and April of the following year). Therefore, to identify permanent and stable aquaculture water surfaces, we only consider Sentinel-2 time-series images captured from April to October. Furthermore, we also tested different composition methods using time-series of the annual water index images from April to October 2019. The comparison of the extraction efficiency of the annual median and mean compositions suggests using the median value to obtain the MNDWI stack images, as it is more accurate in distinguishing the boundaries of the aquaculture ponds.

For the Chinese coastal zone, we use 5856 images in total to obtain the medium stack images, and the corresponding MNDWI threshold is in the -0.2 to 0.2 range. After thresholding the yearly MNDWI medium images of the study area, we generate the resulting water bodies, including the aquaculture ponds and other water bodies such as salt

pans, lakes, rivers, and reservoirs.

Note that in Guangxi province, the use of a single water index time series is not sufficient for extracting the regional water bodies. This is mainly due to the large area of mangrove forests and salt marshes. Hence, the areas with Normalized Difference Vegetation Index (NDVI) greater than 0.01 representing the mangrove areas are excluded first. This is then followed by using MNDWI to extract the coastal water surfaces. NDVI is defined as Eq. (2).

$$\text{NDVI} = (\text{NIR} - \text{Red}) / (\text{NIR} + \text{Red}) \quad (2)$$

3.2. Morphological operations

Utilizing the water index MNDWI and Otsu thresholding method enables us to accurately extract water surfaces from yearly medium stack images. However, the 10 m resolution of Sentinel-2 data cannot fully identify the narrow dikes of aquaculture ponds, which remain in the binarized images of water bodies. In addition, due to the heterogeneity between different water pixels, there are a large number of small holes in the water polygons we extracted. Therefore, a series of morphological operations are required to optimize the morphology of the water bodies.

The binarized water images are generated from GEE and processed in the ERDAS platform. In order to better calculate the biophysical parameters of different water polygons, we first conduct a morphological opening operation to break the weak connections between different water polygons, mainly including the connection of aquaculture ponds and rivers, and meanwhile, eliminate the burr, small protrusions and

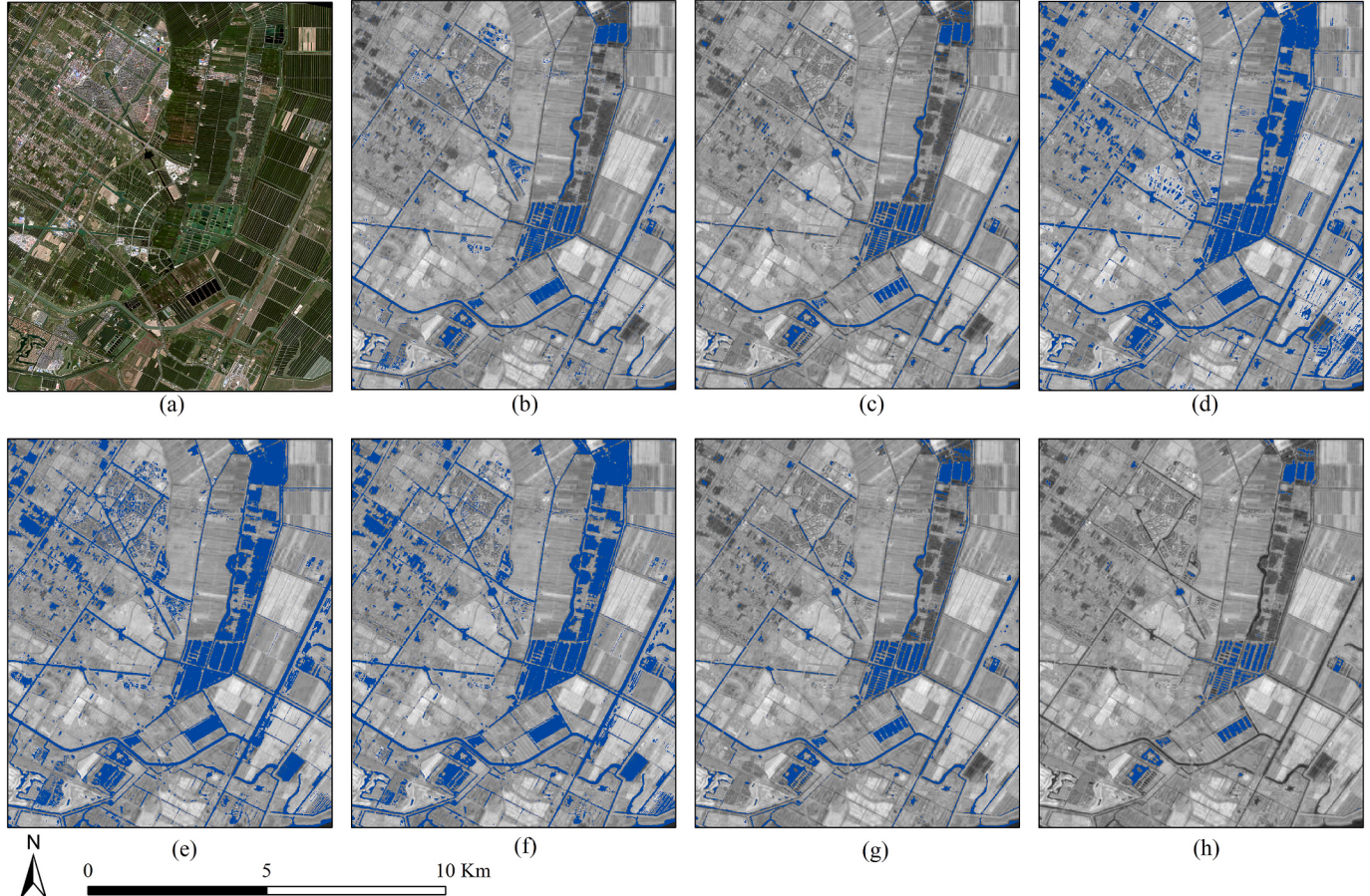


Fig. 3. The extraction result of water bodies using different water indices (a: SuperView-1 Image (R3 G2 B1); b: NDWI (Threshold = -0.06); c: MNDWI (Threshold = 0.17); d: AWEInsh (Threshold = -0.27); e: Aquaculture ponds distribution; f: AWEIsh (Threshold = -0.10); g: WI_2015 (Threshold = -2.52); h: MBWI (Threshold = -0.27)).

some isolated background noise. Then, we use a morphological closing operation to connect similar water bodies and fill the small holes inside the water polygons. The size of kernel is set as 3×3 both in the opening and closing operations.

Among the water bodies we extracted, there are some small water patches, which will affect the extraction accuracy of aquaculture ponds. The spatial analysis tools in ERDAS, namely Clump (Cluster Statistics) and Sieve (Filter Analysis), can be combined to complete the removal of these small patches. The Clump operation identifies the contiguous aquaculture pond pixels whereas Sieve operation eliminates the isolated water patches. The Clump size is set as 8 (use all 8 neighbor pixels) to determine connectivity, the minimum size of Sieve is set as 100 pixels. Using the Clump and Sieve operations, the isolated water patches are removed from the water bodies.

The water bodies after morphological operations have been spatially integrated, so the shape and size of the water patches are no longer suitable for characterizing the morphological characteristics of aquaculture ponds. Therefore, we use the physical parameters of water bodies for further identification of aquaculture ponds.

3.3. Retrieval of biophysical parameters

Satellite remote sensing have been extensively used for monitoring and managing large-scale and long-term variations of water quality (Chen et al., 2019). Water quality parameters, e.g., Chl-a, TSI, and FAI, are bio-indicators of water quality and its biophysical status. The biophysical parameters are estimated based on the spectral reflection characteristics of the water bodies. However, these spectral reflection signals, received by the satellite sensor, are easily affected by phytoplankton, non-algae suspended matter, and Colored Dissolved Organic Matter (CDOM) in the water body because their absorb and/or scatter light (Kondratyev et al., 1998).

Atmospheric correction is necessary when implementing bio-optical models on satellite imagery. This directly affects the retrieval accuracy of water biophysical parameters. The Sentinel-2 Surface Reflectance images available on GEE are pre-processed for atmospheric correction using Sen2Cor. Compared to the water reflectance measured in-situ, the corrected Sentinel-2 surface reflectance product is significantly overestimated. To address this issue, Page et al. (2018) developed an automated site-specific atmospheric correction method that effectively reduces the impact of upper atmospheric noise. Using such an atmospheric correction method, we remove the ozone absorption from the top of the atmosphere reflectance of Sentinel-2A Level-1C data, and then obtain the Rayleigh corrected reflectance (R_{rc}) for the TOA-ozone corrected bands.

3.3.1. Chlorophyll-a

Chlorophyll-a (Chl-a) is often considered as a proxy of the concentration of phytoplankton biomass in different types of water bodies. Therefore, its concentration determines the absorption and scattering characteristics of water bodies. Remote sensing can efficiently retrieve the concentration of Chl-a in water bodies. Mishra and Mishra (2012) proposed a standardized, normalized differential Chlorophyll index (NDCI) to quantitatively monitor the Chl-a concentration from simulated and MEdium Resolution Imaging Spectrometer (MERIS) datasets for inland coastal and estuarine turbid productive (case 2) waters. Their algorithm is also applicable to satellite data and transferable to a wide variety of geographic regions without producing significant uncertainties. Even for remote coastal water bodies without ground truth data, NDCI can efficiently detect algal bloom and qualitatively infers the Chl-a concentration ranges. The NDCI is defined in Eq. (3):

$$NDCI \propto [R_{rs}(708) - R_{rs}(665)] / [R_{rs}(708) + R_{rs}(665)] \quad (3)$$

where $R_{rs}(\lambda)$ is the remote sensing reflectance at wavelength λ . To apply this formula to the Sentinel-2 MSI instrument, we substitute 708 nm

with 705 nm for all atmospheric corrected Sentinel-2 images as in Eq. (4).

$$NDCI \propto [R_{rc}(705) - R_{rc}(665)] / [R_{rc}(705) + R_{rc}(665)] \quad (4)$$

It has been shown that NDCI and Chl-a concentration have a strong correlation with an $R^2 = 0.95$ (Mishra and Mishra, 2012). The polynomial relation between NDCI and the Chl-a measured in-situ is given in Eq. (5).

$$Chl-a = 14.039 + 86.115(NDCI_{Sen2A}) + 194.325(NDCI_{Sen2A})^2 \quad (5)$$

3.3.2. Trophic State Index

The Trophic State Index (TSI) defined by Carlson (1977) characterizes the algal biomass in the water bodies. This index was originally used for the classification of lakes. The Chl-a concentration, Secchi Disk Depth (SDD) and Total Phosphorus (TP) can independently estimate algal biomass and are correlated by linear regression models. Hence, any of those can be theoretically used for the classification of water bodies. Nevertheless, it was shown that Chl-a is often a better predictor for water classification than the other two indices (Carlson, 1983). This is because Chl-a is the most accurate index in predicting algal biomass. The simplified TSI for Chl-a (TSI_{Chl-a}) equation based on Chl-a concentration is presented in Eq. (6):

$$TSI_{Chl-a} = 9.81 \ln(Chl-a) + 30.6 \quad (6)$$

where the Chl-a represents their mean value in water bodies.

3.3.3. Floating Algal Index

Planktonic algae have higher reflectance in the NIR (800 to 900 nm) than that of other wavelengths. Hence, they can be easily distinguished from the surrounding water. Hu (2009) developed an ocean color index, the Floating Algae Index (FAI), to detect the floating algae in various aquatic environments using medium-resolution data from operational MODIS (Moderate Resolution Imaging Spectroradiometer) instruments. This can be also applied to the satellite instruments with similar spectral bands. FAI is defined as the difference between the reflectance at NIR Band (859 nm) and a linear baseline between the Red Band (645 nm) and one of the short-wave infrared bands (i.e., 1240 or 1640 nm):

$$FAI = R_{rc(NIR)} - R'_{rc(NIR)} \\ R'_{rc(NIR)} = R_{rc(RED)} + (R_{rc(SWIR)} - R_{rc(RED)}) (\lambda_{(NIR)} - \lambda_{(RED)}) / (\lambda_{(SWIR)} - \lambda_{(RED)}) \quad (7)$$

where $R_{rc(NIR)}$ ' is the baseline reflectance in the NIR band derived from linear interpolation between the Red and SWIR bands. Comparing to the traditional NDVI (Normalized Difference Vegetation Index) and EVI (Enhanced Vegetation Index), FAI is more advantageous due to its lower sensitivity to variable environments and observing conditions (Hu, 2009). Given the similarity of spectral bands, we extend FAI to Sentinel-2 MSI sensor and set $\lambda_{(NIR)}=842$ nm, $\lambda_{(RED)}=665$ nm and $\lambda_{(SWIR)}=1610$ nm in Eq. (7).

3.4. Time series analysis and optimal threshold

To obtain the threshold of the biophysical parameters suitable for aquaculture ponds extraction, we collected a total of 1200 water samples of different types along the Chinese coastal zone, which include 300 aquaculture ponds, 300 rivers, 300 reservoirs, and 300 salt pans. These water samples comprise 312 in situ field survey samples (256 aquaculture ponds samples, 56 salt pans samples) and 888 samples from high-resolution Google Earth images. The salt pan samples are taken only from locations distributed in the Shandong Province and the north Jiangsu Coastal Plain. The selection of the remaining water samples considers the latitude, randomly distributed on the Chinese coast. Using these water samples, we obtained time series representing the mean

biophysical parameters for each water body type during 2019.

We analyze the time series of biophysical parameters for different water types in Chinese coastal zone. The analysis indicates that the biophysical parameters of aquaculture ponds vary slightly along the Chinese coast. For instance, in Changyi City of Shandong Province, the mean value of Chl-a, TSI, and FAI for aquaculture ponds are 29.34 µg/L, 63.55, and 0.012, respectively (Fig. 4 d, e, f), whereas, in Zhongshan City of Guangdong Province, the mean value of Chl-a, TSI, and FAI for

aquaculture ponds are 57.87 µg/L, 70.06, and 0.025 (Fig. 4 j, k, l).

Nevertheless, the biophysical parameters of aquaculture ponds show a clear distinction from other water types throughout the Chinese coastal zone. In the Pearl River Delta, the average Chl-a for aquaculture ponds, rivers, reservoirs and salt pans are 61.54 µg/L, 8.26 µg/L, 13.76 µg/L, 12.03 µg/L, respectively; the average TSI are 71.26, 51.38, 56.61, 55.76, respectively; and the average FAI are 0.024, -0.012, 0.003, -0.047, respectively. In the Yellow River Delta, the average Chl-a for

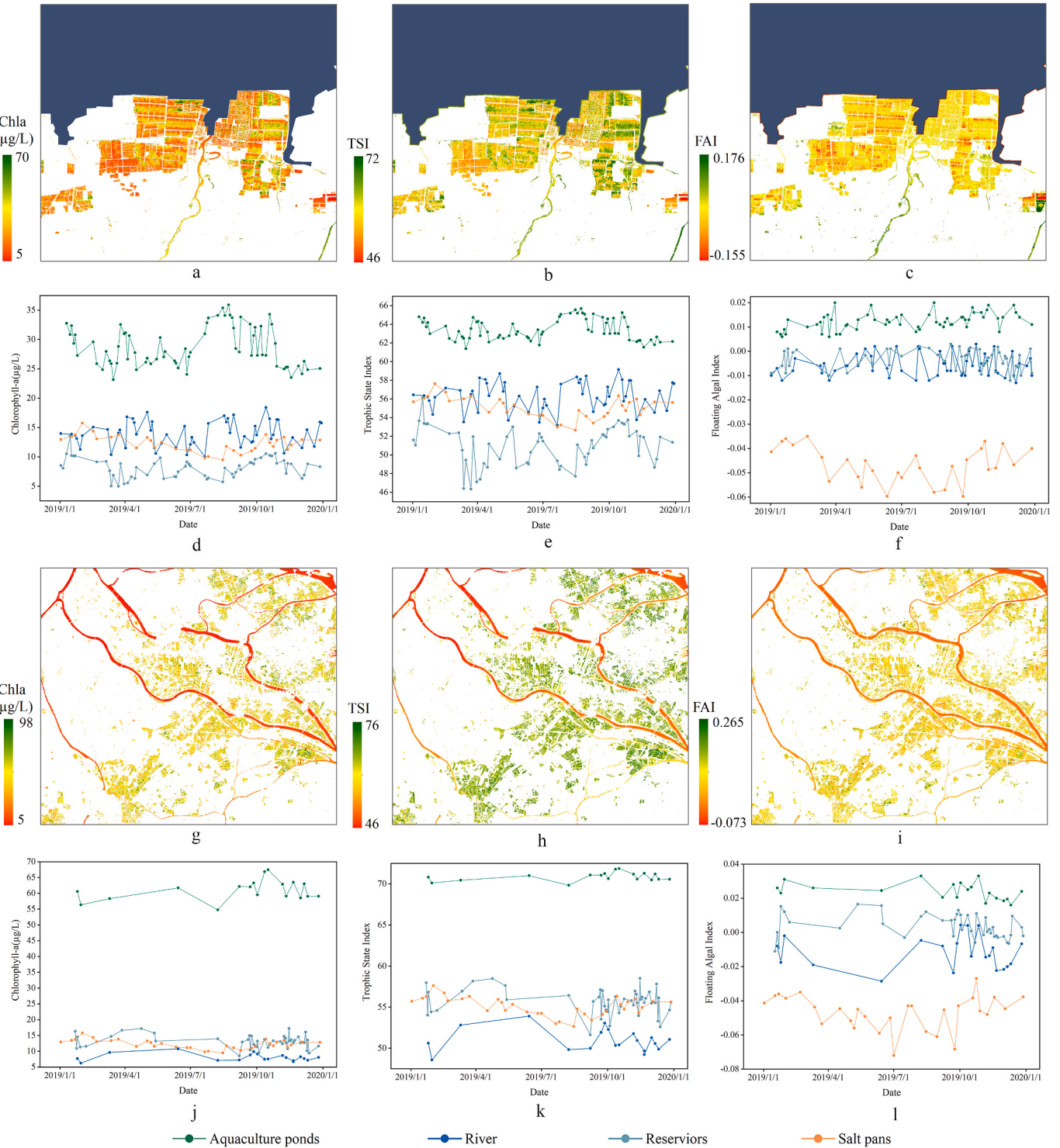


Fig. 4. Map of biophysical parameters in different areas (a-c: Chl-a, TSI, FAI image of the Changyi City; d-f: time series of mean Chl-a, TSI, FAI over different water samples in the Changyi City; g-i: Chl-a, TSI, FAI image of the Zhongshan City; j-l: time series of mean Chl-a, TSI, FAI over different water samples in the Zhongshan City).

aquaculture ponds, rivers, reservoirs and salt pans are 28.05 µg/L, 14.38 µg/L, 8.22 µg/L, 12.68 µg/L; the average TSI are 64.33, 56.97, 51.35, 55.74, and the average FAI are 0.013, -0.006, -0.003, -0.047.

To obtain a transferable threshold, we use the mean biophysical parameters of water bodies in the whole Chinese coastal zone to unify the threshold for aquaculture ponds extraction. In the Chinese coastal zone, the mean Chl-a of aquaculture ponds is 40.54 µg/L, which is much

higher than other water bodies, e.g., rivers (11.32 µg/L), reservoirs (10.52 µg/L), and salt pans (10.37 µg/L). The mean TSI of aquaculture ponds is 60.84, for the rivers, reservoirs, and salt pans, the mean TSI are 54.38, 52.69, 53.40, respectively. The mean FAI of aquaculture ponds is 0.023, for the rivers, reservoirs, and salt pans, the mean FAI are -0.012, 0.000, and -0.047, respectively (see Fig. 5 a, c, e).

To verify the interannual stability of water biophysical parameters,

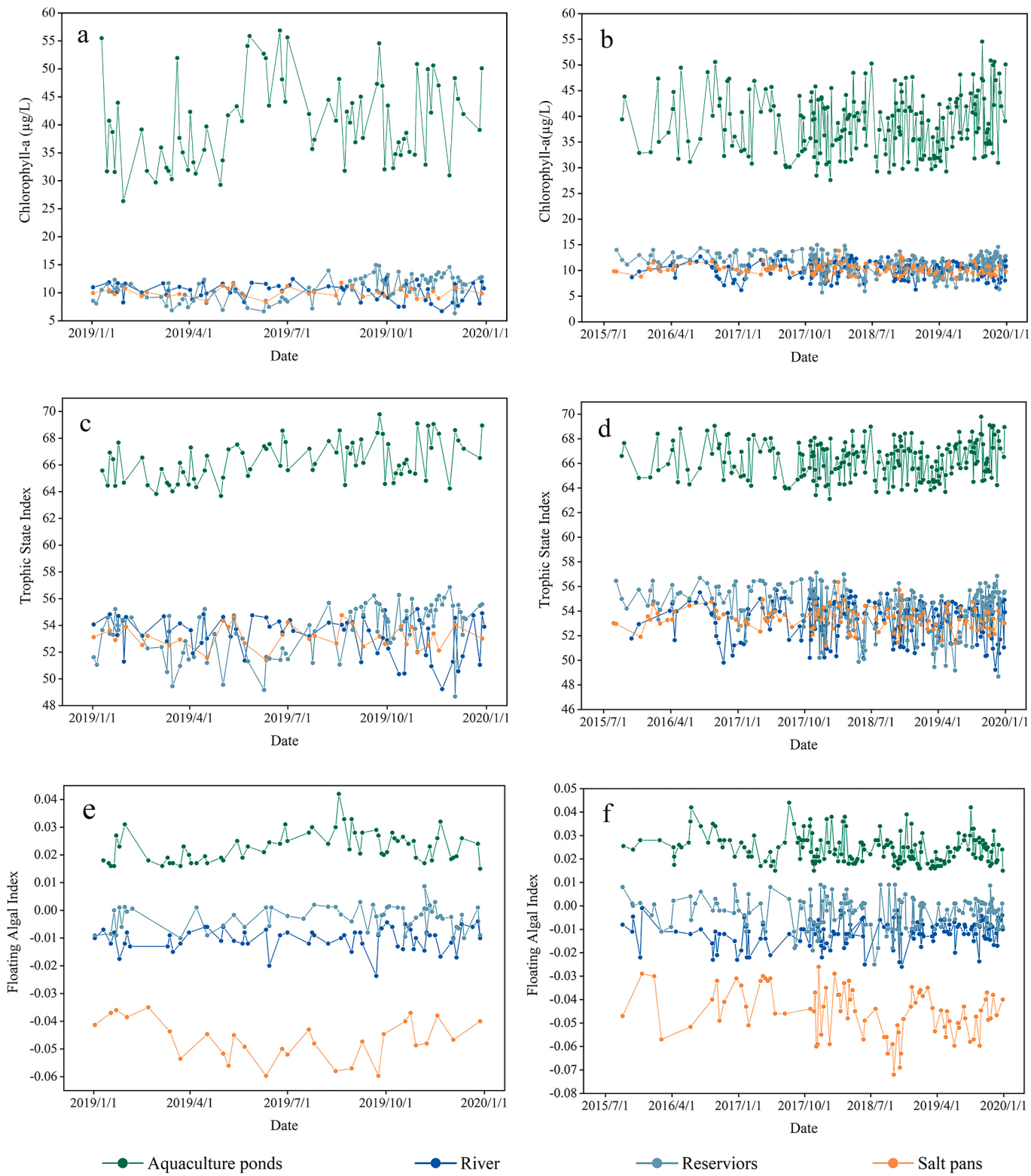


Fig. 5. Time series of biophysical parameters for different Chinese coastal water bodies (a, c, e: 2019; b, d, f: 2015–2019).

we also calculate the time series of the mean Chl-a, TSI, FAI in 2015–2019 (Fig. 5 b, d, f). These time series indicate that Chl-a, TSI, FAI also provide a clear distinction for aquaculture ponds, lakes, rivers, and salt pans, and demonstrate high stability on a four-year scale.

In this paper, we set the water biophysical parameters thresholds for Chl-a, TSI, FAI to 25.03 µg/L, 56.35, and 0.010, respectively, to efficiently distinguish aquaculture ponds from other types of water bodies.

3.5. Aquaculture ponds extraction

Based on the water index and thresholding method and using bio-optical models, we obtained images of yearly medium, mean Chl-a, mean TSI, and mean FAI of coastal water bodies. Since the water pixels in aquaculture ponds are heterogeneous, the biophysical parameters vary in a single aquaculture pond polygon. Therefore, we first use the Zonal Statistics tool in ArcGIS to calculate the average biophysical parameters for each water polygon. A decision tree is then established to extract the coastal aquaculture ponds based on the previously obtained

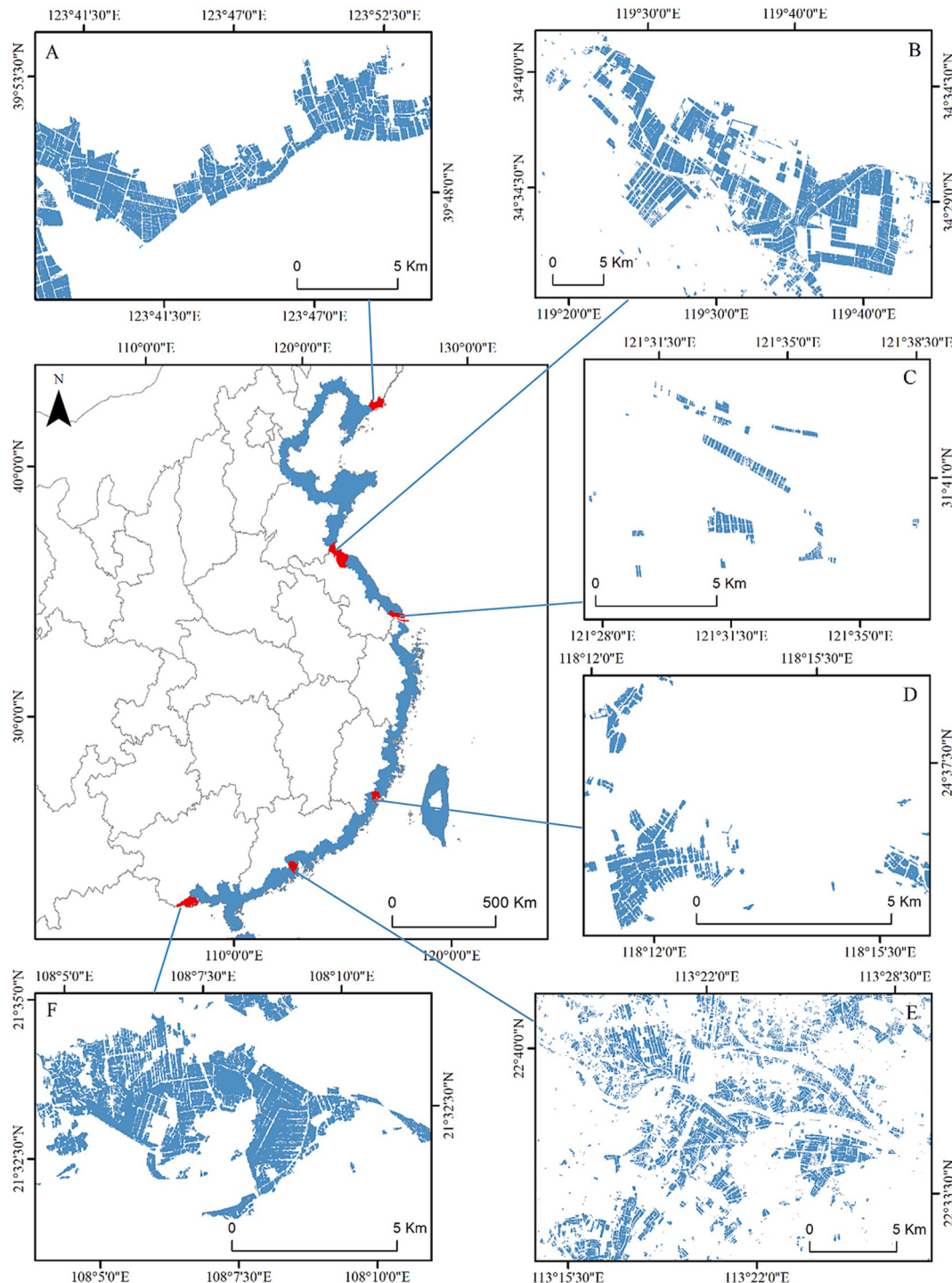


Fig. 6. The extraction result of aquaculture ponds in different regions of the China coast (A: Dandong City; B: Lianyungang City; C: Shanghai City; D: Xiamen City ; E : Zhongshan City ; F: Fangchenggang City).

threshold.

The preliminary aquaculture ponds we extracted include some narrow rivers connected to the aquaculture ponds and a small number of lakes, and reservoirs with high trophic status. For these water bodies that are completely different from aquaculture ponds in their geometric features, we manually removed them from the results (Fig. 6).

4. Result

4.1. Accuracy assessment and verification

To verify the accuracy of the proposed aquaculture ponds extraction method, we use the confusion matrix on a local and national scale, respectively. We consider three major local verification areas, namely the Yellow River Estuary, North Jiangsu Coastal Plain, and Pearl River Estuary. Using the Fishnet tool (0.2×0.2 cell size) in ArcGIS, 882 random points are generated to cover the considered study areas. Each verification point is divided into aquaculture and non-aquaculture. The 882 random points included 336 aquaculture points and 546 non-aquaculture points. The validation datasets are built using the UAV-

based data collection and high-resolution Google Earth imagery. The results indicate that the national-scale accuracy is 91 %, with a Kappa coefficient of 0.83.

In the Yellow River Estuary, the overall accuracy of our aquaculture ponds extraction method is 85 % with Kappa coefficient of 0.81. In the northern Jiangsu province, the overall accuracy is 89 % with Kappa coefficient of 0.78. In the Pearl River Estuary, the overall accuracy is 95 % with Kappa coefficient of 0.85. The proposed method has its highest accuracy in the Pearl River Estuary. This is due to the large difference between the biophysical parameters of aquaculture ponds and other water bodies present there.

4.2. Spatial distribution of coastal aquaculture ponds

Based on time series of Sentinel-2 images and biophysical parameters, we carried out a comprehensive analysis of the Chinese coastal aquaculture ponds. The data is projected using the Asia North Albers Equal Area Conic project in ArcGIS.

Our findings indicate that the total area of aquaculture ponds in the Chinese coastal zone was 1,039,214 ha in 2019, accounting for about

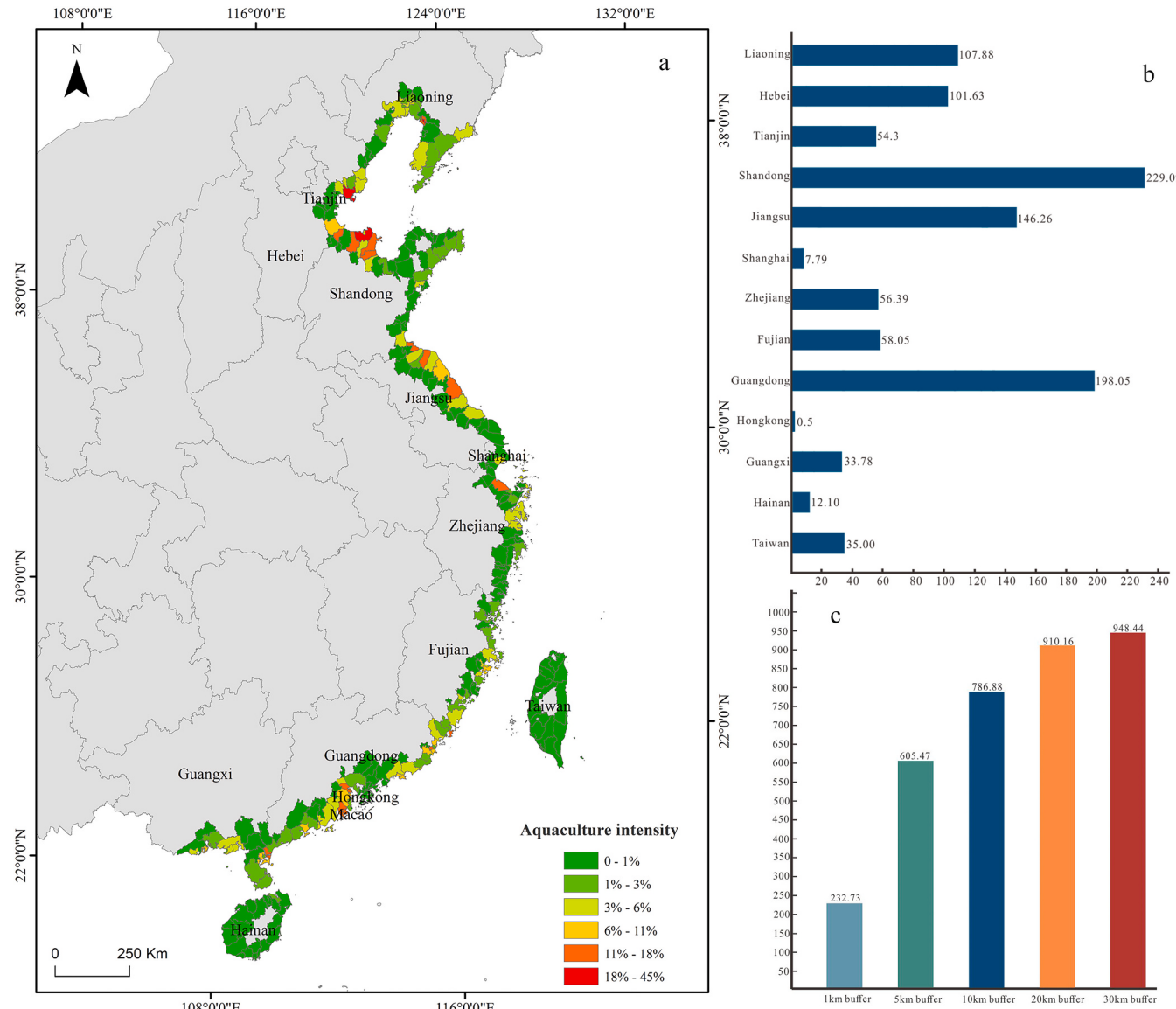


Fig. 7. Chinese coastal aquaculture ponds distribution (a: spatial distribution and intensity of aquaculture ponds; b: aquaculture area of different provinces expressed in 10^3 ha; c: the aquaculture intensity of different coastal buffer zones expressed in 10^3 ha).

14.6 % of the total aquaculture area in China. It is also seen that more than 55 % of aquaculture ponds are concentrated in the Yellow River Estuary, the North Jiangsu Coastal Plain, and the Pearl River Estuary. The largest number of Chinese coastal aquaculture ponds is in Shandong province with a total area of 227,493 ha, representing 22 % of the total number of Chinese coastal aquaculture ponds. Guangdong Province has the second largest number of aquaculture ponds, with a total area of 198,052 ha, which is about 19 % of Chinese coastal aquaculture ponds (Fig. 7 b).

Furthermore, we calculated the aquaculture intensity (i.e., the ratio of aquaculture ponds area to the total administrative area) of Chinese coastal zone. The top three provinces in aquaculture intensity are Hebei Province, Jiangsu Province, and Shandong Province with aquaculture intensities of 8.52 %, 6.35 % and 5.08 %, respectively. Among the 311 districts analyzed, the ones with the highest aquaculture intensity were mostly concentrated in the cities of Dongying and Binzhou (Shandong Province), Lianyungang and Yancheng (Jiangsu Province), and Zhuhai and Zhongshan (Guangdong Province) (Fig. 7 a).

To analyze the intensity of aquaculture ponds at different distances from the coastline, we further considered inshore buffers of 1 km, 5 km, 10 km, 20 km, and 30 km from the Chinese administration coastline. The total area of aquaculture ponds in the five buffers were 232,728 ha; 605,466 ha; 786,884 ha; 910,160 ha; and 948,437 ha, respectively. The highest aquaculture intensity is in the 1-km coastal buffer zone, reaching 22.4 % of the total Chinese coastal aquaculture ponds. Also, about 58 % of the aquaculture ponds are concentrated in the 0–5 km buffer zone. As the distance increases, the intensity of aquaculture gradually decreases. Within 20 to 30 km, the aquaculture intensity decreases to the minimum, covering only 38,277 ha (Fig. 7 c).

5. Discussion

5.1. Selection of the chlorophyll-a retrieval algorithm

There exist several methods for retrieving Chl-a concentrations on different types of waters bodies using various satellite data. Due to the intrinsic complexity of coastal ecosystems and the optical characteristics of coastal water, it is however challenging to construct a standardized methodological framework applicable at different spatial scales. The anthropological properties of coastal aquaculture ponds only add extra difficulty to Chl-a retrieval algorithms.

Neil et al. (2019) studied 48 Chl-a retrieval algorithms that are currently available worldwide and ranked their retrieval accuracy. To select the most accurate Chl-a retrieval model for the Chinese coastal zone, we examined the top 6 algorithms with the highest scores (Supplementary Table 1). Our investigation indicates that the retrieval algorithms established on 665 nm and 705 nm wavelengths are more efficient in retrieving Chl-a concentrations in our study area. We collected 100 sets of different field survey water samples in the coastal zone of China, and measured the in-situ water spectrum characteristics using the ASD-HH2 handheld portable spectrometer (spectral range 350–1075 nm). The Sentinel-2 spectral response function was used to simulate the equivalent spectrum of the measured spectrum. This is then converted to the equivalent remote sensing reflectance in the corresponding band. Furthermore, we collected the 100 sets of water samples from the field and tested the Chl-a concentrations in the laboratory. The Chl-a concentration was extracted using 90 % cool acetone, and then measured using a fluorimeter (Trilogy, Turner Design, CA, USA). Based on the Chl-a concentrations measured in the laboratory and the water spectrum values, we then carried out a fitting experiment. Our analysis shows that the algorithm proposed by Mishra and Mishra (2012) is more efficient in highlighting the aquaculture waters, lakes, reservoirs, and salt pans (Fig. 8 Model D). Therefore, we selected this algorithm to perform the bio-optical retrieval on the coastal water bodies.

5.2. Relationship between biophysical parameters and aquaculture species

The main aquaculture species in China are fish, crustaceans, and mollusks. Fish is the dominant product whether in the coastal zone or inland (China Fishery Statistical Yearbook, 2020; FAO, 2020). The water quality of aquaculture ponds is closely related to the aquaculture species. The middle and late aquaculture stages of fish and shrimp are often in the high-temperature season. The rising temperature and accumulation of organic matter such as bait and feces, increase the intensity of planktonic algae in the ponds resulting in a high nutritional status. Sea cucumber aquaculture ponds, however, have strict requirements on their aquaculture environment. The algae in the aquaculture ponds need to be cleaned regularly to prevent the water quality from deteriorating. Therefore, the biophysical parameters of sea cucumber aquaculture ponds are lower than other aquaculture ponds.

According to the yearbook data and our field investigations, we established a database of the main aquaculture species in different provinces and regions of China. It is seen that Jiangsu province has the highest mollusks and algae production. Shandong province has a large area of sea cucumber aquaculture ponds which are mainly distributed in the Yellow River Delta.

We also analyzed the mean value of biophysical parameters in the Chinese coastal provinces. The results indicate that the biophysical parameters of aquaculture ponds in the Chinese coastal zone show subtle variances in different regions. For instance, in the Yellow River Estuary, the mean value of Chl-a, TSI, and FAI of aquaculture ponds were 21.73 µg/L, 56.15, and 0, respectively. In the North Jiangsu Coastal Plain, the mean value of Chl-a, TSI, and FAI of aquaculture ponds were 37.23 µg/L, 64.19, and 0.03 respectively. Furthermore, in the Changjiang River Estuary, the mean values were 26.63 µg/L, 60.18, 0.03, respectively, and in the Pearl River Estuary, the mean values were 27.18 µg/L, 61.80, and 0.03 respectively. The biophysical parameters of aquaculture ponds in the Yellow River Delta have the lowest Chl-a, TSI, and FAI values among all the districts in China. This is attributed to the large-scale sea cucumber aquaculture ponds in this area. Jiangsu province, however, has the highest biophysical parameters due to its abundance of mollusks and algae production.

5.3. Limitations and application

The heterogeneity of coastal biophysical morphology and anthropogenic intervention are the main challenging factors in mapping coastal aquaculture ponds. Although we can recognize biophysical parameters in different types of water bodies, the boundary of the aquaculture ponds is partly connected to the river boundaries. These connected water polygons need to be divided manually, which increases the difficulty of the aquaculture ponds extraction. Furthermore, there are some isolated regular water patches with high trophic status in the Chinese coastal zone, we cannot accurately determine whether these small water bodies are used for aquaculture in the post-processing procedure. This leads to an uncertainty of the results of the aquaculture ponds.

Compared to the method presented in Duan et al. (2020), our proposed method perfectly distinguishes aquaculture ponds without the need to manually remove the salt pans and other natural water bodies with similar geometric features. However, our method can only be used in regions where the water contained with aquaculture ponds cannot be exchanged with the surrounding seawater, i.e., high tide aquaculture ponds that are “non-submerged area” (Virdis, 2014), as the frequent exchange of aquaculture water with seawater changes the biophysical parameters of aquaculture ponds. And meanwhile, there are also a small number of aquaculture ponds with better water quality control whose mean biophysical parameters are not significantly higher than those of natural water bodies in Chinese coastal zone. The existence of these aquaculture ponds causes our extraction results to be underestimated.

Our results show the effectiveness of remotely sensed biophysical

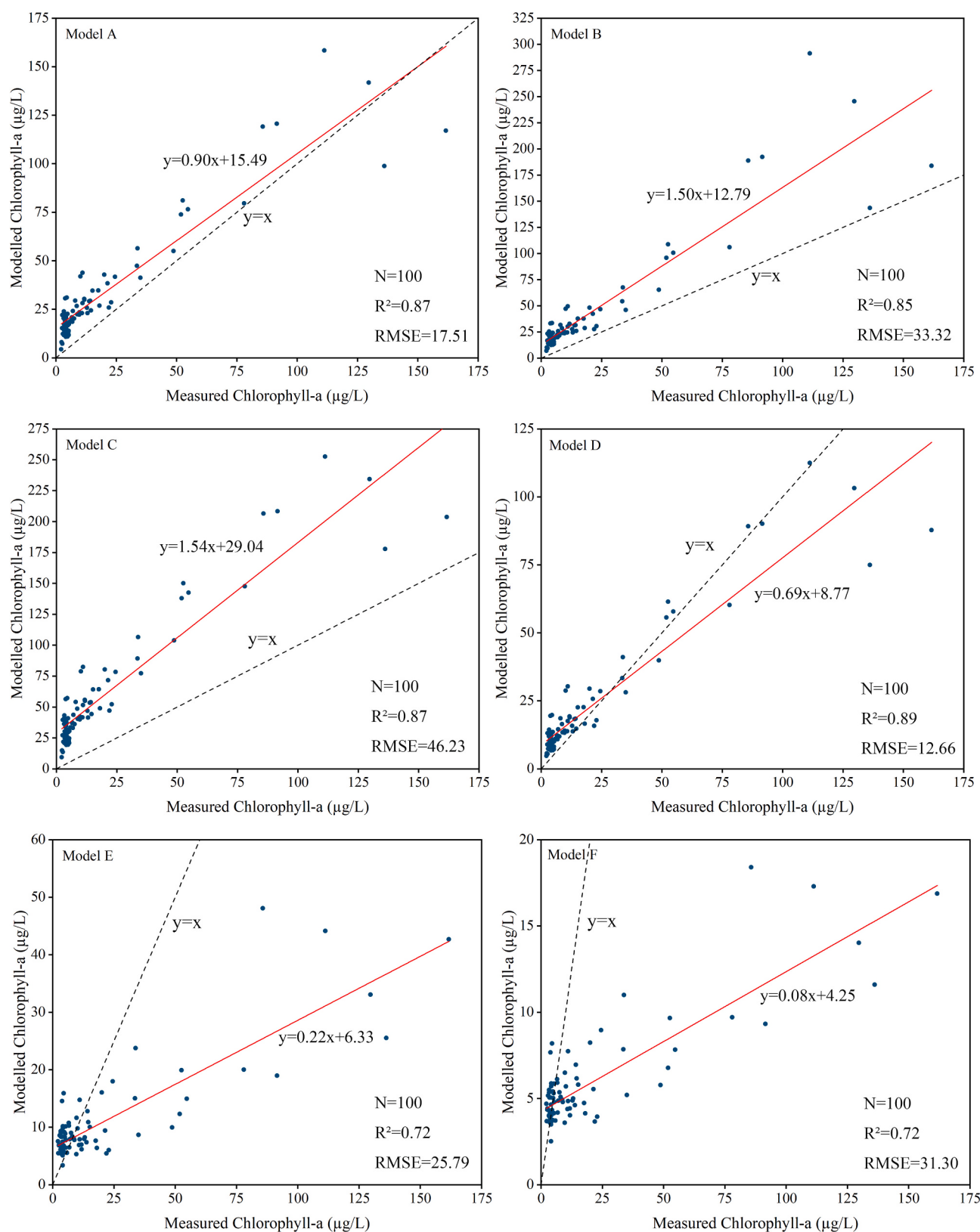


Fig. 8. Comparison of model and in-situ measurement of Chlorophyll-a concentrations conducted over the Chinese coastal zone. (R^2 : correlation coefficient; RMSE: root mean square error; red solid line: best-fit line; blue dashed line: $y = x$ line). (For interpretation of the references to color in this figure legend, the reader is referred to the web version of this article.)

parameters to accurately identify coastal aquaculture ponds from Sentinel-2 time series images in GEE. There are significant differences in biophysical parameters of the aquaculture ponds for different aquaculture species. Therefore, our method has great potential in the classification of the aquaculture species.

6. Conclusion

With growing demand in aquatic food and nutrition, it has become extremely important to track and monitor the expansion of aquaculture facilities at the fragile coastal frontier. In this paper, we examine a 30 km buffer zone of the Chinese administration coastline and use more than 5856 Sentinel-2 images to build a novel aquaculture ponds identification method. Our proposed method combines the spatial characteristics with biophysical parameters derived from bio-optical models in the GEE platform. The proposed method effectively distinguishes coastal aquaculture ponds from other water bodies with similar shapes and achieves a 91 % overall accuracy with a Kappa coefficient of 0.83.

The total area of aquaculture ponds in the Chinese coastal zone in 2019 was 1,039,214 ha. These were mainly distributed in Shandong and Guangdong provinces, which contain low-lying plains and estuaries suitable for aquaculture development. The 0–5 km buffer zone from the Chinese coastline has the largest aquaculture intensity, with 58 % of the total aquaculture ponds in the Chinese coastal zone. Further away from the coast, the intensity of the aquaculture ponds decreases, and in the 30 km buffer zone, the area of aquaculture ponds reaches its maximum value and keeps stable.

Furthermore, our study provides a new perspective in distinguishing different water types using biophysical parameters that reflect the internal characteristics of water pixels. The differences in the biophysical parameters of Chinese coastal aquaculture ponds is closely related to the aquaculture species. The North Jiangsu coastal plain has the highest Chl-a concentration and TSI values due to its highest mollusks and algae production. Shandong Province has relatively lower biophysical parameters due to its large areas of sea cucumber aquaculture ponds that have strict water quality requirements. Our results indicate that the biophysical parameters are promising indicators for distinguishing the aquaculture species and can be adopted in future studies.

Supplementary data to this article can be found online at <https://doi.org/10.1016/j.marpolbul.2022.113901>.

CRediT authorship contribution statement

Ya Peng: Conceptualization, Methodology, Code writing, Investigation, Writing-original draft preparation, Writing-Reviewing and Editing. **Dhriraj Sengupta:** Methodology, Code writing, Writing-review & editing. **Yuanqiang Duan:** Investigation, Writing-Reviewing. **Chunpeng Chen:** Investigation, Writing-Reviewing. **Bo Tian:** Writing-review & editing.

Declaration of competing interest

The authors declare that they have no known competing financial interests or personal relationships that could have appeared to influence the work reported in this paper.

Data availability

Data will be made available on request.

Acknowledgements

This work is supported by the National Key Research and Development Program of China (No. 2018YFE0101000) and the National Natural Science Foundation of China (No. 42030402, 51739005).

References

- Carlson, R.E., 1977. A trophic state index for lakes. *Limnol. Oceanogr.* 22, 361–369.
- Carlson, R.E., 1983. DISCUSSION: "Using Differences Among Carlson's Trophic State Index Values in Regional Water Quality Assessment," by Richard A. Osgood. *J. Am. Water Resour. Assoc.* 19, 307–308.
- Chen, X., Shang, S., Lee, Z., Qi, L., Yan, J., Li, Y., 2019. High-frequency observation of floating algae from AHI on Himawari-8. *Remote Sens. Environ.* 227, 151–161.
- Chen, W., Wang, D., Huang, Y., Chen, L., Zhang, L., Wei, X., Sang, M., Wang, F., Liu, J., Hu, B., 2017. Monitoring and analysis of coastal reclamation from 1995–2015 in Tianjin Binhai New Area, China. *Sci. Rep.* 7, 1–12.
- China Fishery Statistical Yearbook, 2020. China Agriculture Press, Beijing, China, pp. 24–34.
- Duan, Y., Li, X., Zhang, L., Chen, D., Ji, H., 2020. Mapping national-scale aquaculture ponds based on the Google Earth Engine in the Chinese coastal zone. *Aquaculture.* 520, 734666.
- Duan, Y., Tian, B., Li, X., Liu, D., Sengupta, D., Wang, Y., Peng, Y., 2021. Tracking changes in aquaculture ponds on the China coast using 30 years of landsat images. *Int. J. Appl. Earth Obs. Geoinf.* 102, 102383.
- FAO, 2020. The State of World Fisheries and Aquaculture 2020. Sustainability in Action. Rome.
- Feyisa, G.L., Meilby, H., Fensholt, R., Proud, S.R., 2014. Automated water extraction index: a new technique for surface water mapping using landsat imagery. *Remote Sens. Environ.* 140, 23–35.
- Fisher, A., Flood, N., Danaher, T., 2016. Comparing landsat water index methods for automated water classification in eastern Australia. *Remote Sens. Environ.* 175, 167–182.
- Føre, M., Frank, K., Norton, T., Svendsen, E., Alfredsen, J.A., Dempster, T., Eguiraun, H., Watson, W., Stahl, A., Sunde, L.M., Schellewald, C., Skjøen, K.R., Alver, M.O., Berckmans, D., 2018. Precision fish farming: A new framework to improve production in aquaculture. *Biosyst. Eng.* 173, 176–193.
- Hu, C., 2009. A novel ocean color index to detect floating algae in the global oceans. *Remote Sens. Environ.* 113, 2118–2129.
- Kondratyev, K.Y., Pozdnjakov, D.V., Pettersson, L.H., 1998. Water quality remote sensing in the visible spectrum. *Int. J. Remote Sens.* 19, 957–979.
- Louis, J., Pflug, B., Main-Knorn, M., Debaecker, V., Mueller-Wilm, U., Iannone, R.Q., Cadau, E.G., Boccia, V., Gascon, F., 2019. Sentinel-2 global surface reflectance level-2A product generated with Sen2Cor. In: IGARSS 2019–2019 IEEE International Geoscience and Remote Sensing Symposium. IEEE, pp. 8522–8525.
- McFeeters, S.K., 1996. The use of the normalized difference water index (NDWI) in the delineation of open water features. *Int. J. Remote Sens.* 17, 1425–1432.
- Merkens, J.L., Reimann, L., Hinkel, J., Vafeidis, A.T., 2016. Gridded population projections for the coastal zone under the shared socioeconomic pathways. *Glob. Planet. Chang.* 145, 57–66.
- Mishra, S., Mishra, D.R., 2012. Normalized difference chlorophyll index: a novel model for remote estimation of chlorophyll-a concentration in turbid productive waters. *Remote Sens. Environ.* 117, 394–406.
- Neil, C., Spyralos, E., Hunter, P.D., Tyler, A.N., 2019. A global approach for chlorophyll-a retrieval across optically complex inland waters based on optical water types. *Remote Sens. Environ.* 229, 159–178.
- Otsu, N., 1979. A threshold selection method from gray-level histograms. *IEEE Trans. Syst. Man and Cybernetics.* 9, 62–66.
- Ottinger, M., Clauss, K., Kuenzer, C., 2016. Aquaculture: relevance, distribution, impacts and spatial assessments – a review. *Ocean Coast. Manag.* 119, 244–266.
- Ottinger, M., Clauss, K., Kuenzer, C., 2017. Large-scale assessment of coastal aquaculture ponds with sentinel-1 time series data. *Remote Sens.* 9, 440.
- Ottinger, M., Clauss, K., Huth, J., Eisfelder, C., Leinenkugel, P., Kuenzer, C., 2018. Time series sentinel-1 SAR data for the mapping of aquaculture ponds in coastal Asia. In: IGARSS 2018–2018 IEEE International Geoscience and Remote Sensing Symposium. IEEE, pp. 9371–9374.
- Páez-Osuna, F., 2001. The Environmental Impact of Shrimp Aquaculture: A Global Perspective. *Environ. Pollut.* 112, 229–231.
- Page, B.P., Kumar, A., Mishra, D.R., 2018. A novel cross-satellite based assessment of the spatio-temporal development of a cyanobacterial harmful algal bloom. *Int. J. Appl. Earth Obs. Geoinf.* 66, 69–81.
- Peng, Y., Chen, G., Li, S., Liu, Y., Pernetta, J.C., 2013. Use of degraded coastal wetland in an integrated mangrove-aquaculture system: a case study from the South China Sea. *Ocean Coast. Manag.* 85, 209–213.
- Ren, C., Wang, Z., Zhang, Y., Zhang, B., Chen, L., Xi, Y., Xiao, X., Doughty, R.B., Liu, M., Jia, M., Mao, D., Song, K., 2019. Rapid expansion of coastal aquaculture ponds in China from Landsat observations during 1984–2016. *Int. J. Appl. Earth Obs. Geoinf.* 82, 101902.
- Sohel, M.S.I., Ullah, M.H., 2012. Ecohydrology: a framework for overcoming the environmental impacts of shrimp aquaculture on the coastal zone of Bangladesh. *Ocean Coast. Manag.* 63, 67–78.
- Spalding, M., McIvor, A., Tonneijck, F., Tol, S., Eijk, P.v., 2014. Mangroves for Coastal Defence.
- SRTM, 2017. 90m Digital Elevation Database v4.1. CGIAR-CSI URL. <https://cgarsci.community/data/srtm-90m-digital-elevation-database-v4-1/>. (Accessed 1 January 2021).
- Sun, Z., Luo, J., Yang, J., Yu, Q., Zhang, L., Xue, K., Lu, L., 2020. Nation-scale Mapping of Coastal Aquaculture Ponds With Sentinel-1 SAR Data Using Google Earth Engine. *Remote Sens.* 12, 3086.
- Tran, H., Tran, T., Kervyn, M., 2015. Dynamics of land cover/land use changes in the Mekong Delta, 1973–2011: A remote sensing analysis of the Tran Van Thoi District, Ca Mau Province, Vietnam. *Remote Sens.* 7, 2899–2925.

- Virdis, S.G.P., 2014. An object-based image analysis approach for aquaculture ponds precise mapping and monitoring: a case study of Tam Giang-Cau Hai Lagoon, Vietnam. *Environ. Monit. Assess.* 186, 117–133.
- Waite, R., Beveridge, M., Brummett, R., Castine, S., Chaiyawannakarn, N., Kaushik, S., Mungkun, R., Nawapakpilai, S., Phillips, M., 2014. Improving productivity and environmental performance of aquaculture. World Resources Institute.
- Wang, W., Liu, H., Li, Y., Su, J., 2014. Development and management of land reclamation in China. *Ocean Coast. Manag.* 102, 415–425.
- Wang, X., Xie, S., Zhang, X., Chen, C., Guo, H., Du, J., Duan, Z., 2018. A robust multi-band water index (MBWI) for automated extraction of surface water from landsat 8 OLI imagery. *Int. J. Appl. Earth Obs. Geoinf.* 68, 73–91.
- Xia, Z., Guo, X., Chen, R., 2020. Automatic extraction of aquaculture ponds based on Google earth engine. *Ocean Coast. Manag.* 198, 105348.
- Xu, H., 2006. Modification of normalised difference water index (NDWI) to enhance open water features in remotely sensed imagery. *Int. J. Remote Sens.* 27, 3025–3033.
- Yao, Y., Ren, C., Wang, Z., Wang, C., Deng, P., 2016. Monitoring of Salt Ponds and Aquaculture Ponds in the Coastal Zone of China in 1985 and 2010. *Wetl. Sci.* 14, 874–882.
- Ying, Z., Wu, J., Del Valle, T.M., Yang, W., 2020. Spatiotemporal dynamics of coastal aquaculture and driving force analysis in Southeastern China. *Ecosyst Health Sust.* 6, 1851145.
- Zeng, Z., Wang, D., Tan, W., Yu, G., You, J., Lv, B., Wu, Z., 2021. RCSANet: A Full Convolutional Network for Extracting Inland Aquaculture Ponds from High-Spatial-Resolution Images. *Remote Sens.* 13, 92.